USGS
science for a changing world

Species Management Research Program

Prepared in cooperation with the Western Association of Fish and Wildlife Agencies and the Bureau of Land Management

Range-wide Population Trend Analysis for Greater Sage-Grouse (*Centrocercus urophasianus*)—Updated 1960–2021

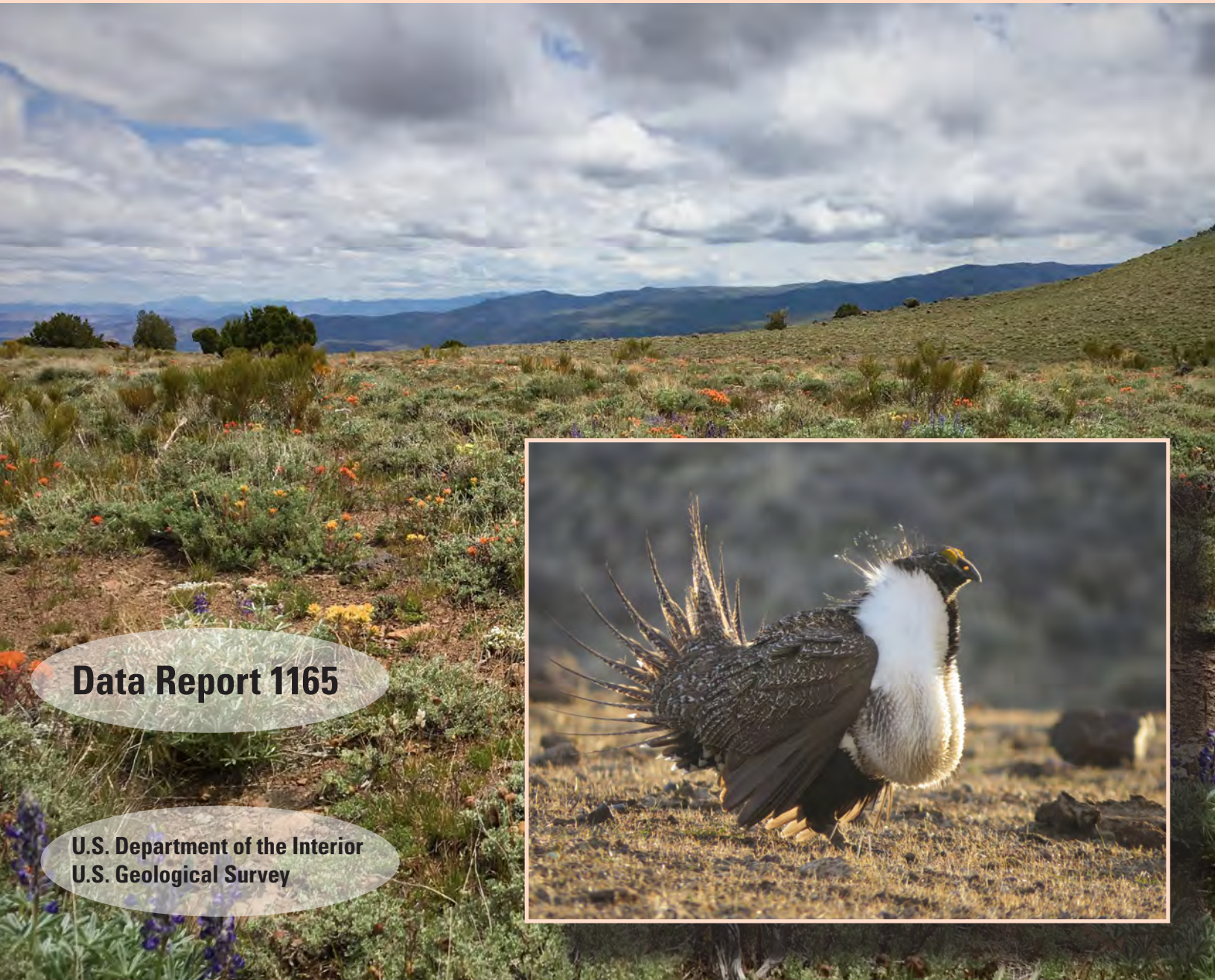

Data Report 1165

U.S. Department of the Interior
U.S. Geological Survey

Cover. Sagebrush steppe flora in the Fort Sage Mountains of Nevada and California, USA. Photograph by Emmy A. Tyrrell, U.S. Geological Survey, May 21, 2018.

Inset: Male greater sage-grouse (*Centrocercus urophasianus*) displaying on lek. Photograph by Sarah McIntire, University of Idaho, March 24, 2018, used with permission.

Range-wide Population Trend Analysis for Greater Sage-Grouse (*Centrocercus urophasianus*)—Updated 1960–2021

By Peter S. Coates, Brian G. Prochazka, Cameron L. Aldridge, Michael S. O'Donnell, David R. Edmunds, Adrian P. Monroe, Steve E. Hanser, Lief A. Wiechman, and Michael P. Chenaille

Species Management Research Program

Prepared in cooperation with the Western Association of Fish and Wildlife Agencies and the Bureau of Land Management

Data Report 1165

U.S. Department of the Interior
U.S. Geological Survey

U.S. Geological Survey, Reston, Virginia: 2022

Suggested citation:
Coates, P.S., Prochazka, B.G., Aldridge, C.L., O'Donnell, M.S., Edmunds, D.R., Monroe, A.P., Hanser, S.E., Wiechman, L.A., and Chenaille, M.P., 2022, Range-wide population trend analysis for greater sage-grouse (*Centrocercus urophasianus*)—Updated 1960–2021: Data Report 1165, 16 p., https://doi.org/10.3133/dr1165.

Associated data for this publication:
Coates, P.S., Prochazka, B.G., Aldridge, C.L., O'Donnell, M.S., Edmunds, D.R., Monroe, A.P., Hanser, S.E., Wiechman, L.A., and Chenaille, M.P., 2022, Trends and a targeted annual warning system for greater sage-grouse in the western United States (1960–2021): U.S. Geological Survey data release, https://doi.org/10.5066/P9OQWGIV.

ISSN 2771-9448 (online)

Acknowledgments

We conducted this update and original modeling analysis in close consultation with the Bureau of Land Management, Sage-Grouse and Columbian Sharp-tailed Grouse Technical Committee for the Western Association of Fish and Wildlife Agencies, and the U.S. Fish and Wildlife Service. We thank John Tull (U.S. Fish and Wildlife Service) and Robert Arkle (U.S. Geological Survey) for helpful comments in reviewing this data report in its entirety. We extend gratitude for the cooperation of personnel from 11 western state wildlife agencies, who provided feedback at various stages on uses of lek data, modeling methods, and constructive reviews at various stages of production. Specifically, we value the contributions from T. Remington (Western Association of Fish and Wildlife Agencies), S. Stiver (Western Association of Fish and Wildlife Agencies), S. Espinosa (Nevada Department of Wildlife), K. Griffin (Colorado Parks and Wildlife), K. Miller (California Department of Fish and Wildlife), A. Moser (Idaho Department of Fish and Game), A. Cook (Utah Division of Wildlife Resources), L. Foster (Oregon Department of Fish and Wildlife), J. Kolar (North Dakota Game and Fish Department), T. Runia (South Dakota Department of Game, Fish and Parks), M. Schroeder (Washington Department of Fish and Wildlife), N. Whitford (Wyoming Game and Fish Department), C. Wightman (Montana Department of Fish, Wildlife and Parks), B. Wakeling (Montana Department of Fish, Wildlife and Parks), S. Vold (Oregon Department of Fish and Wildlife), and M. Cline (Oregon Department of Fish and Wildlife). We thank K. Andrle (Nevada Department of Wildlife), K. McGowan, M. Magaletti, A. Kosic, P. Winters (Bureau of Land Management), J. Tull (U.S. Fish and Wildlife Service), K. Borland, M. Nelson (U.S. Forest Service), S. Abele (U.S. Fish and Wildlife Service), S. Gardner, and B. Ehler (California Department of Fish and Wildlife) for their input throughout the initial components of this study. This project could not have been completed without the financial support of the Bureau of Land Management, U.S. Geological Survey, and the funds for the pilot efforts that were provided by the Bureau of Land Management-Nevada and Nevada Department of Wildlife.

Contents

Figures

Tables

Conversion Factors

International System of Units to U.S. customary units

Multiply	By	To obtain
	Length	
kilometer (km)	0.6214	mile (mi)
	Area	
hectare (ha)	2.471	acre
hectare (ha)	0.003861	square mile (mi^2)

Datum

Vertical coordinate information is referenced to the North American Vertical Datum of 1988 (NAVD 88).

Horizontal coordinate information is referenced to the World Geodetic System (WGS 84).

Elevation, as used in this report, refers to distance above the vertical datum.

Abbreviations

$\widehat{N}$	estimated abundance
$\hat{r}$	estimated intrinsic rate of population change
$\hat{\lambda}$	estimated finite rate of population change
BLM	Bureau of Land Management
CC	climate cluster
CRI	credible interval
MCMC	Markov chain Monte Carlo
N	abundance
NC	neighborhood cluster
QA/QC	quality assessment and quality control
SSM	state-space model
USGS	U.S. Geological Survey
WAFWA	Western Association of Fish and Wildlife Agencies

Range-wide Population Trend Analysis for Greater Sage-Grouse (*Centrocercus urophasianus*)—Updated 1960–2021

By Peter S. Coates, Brian G. Prochazka, Cameron L. Aldridge, Michael S. O'Donnell, David R. Edmunds, Adrian P. Monroe, Steve E. Hanser, Lief A. Wiechman, and Michael P. Chenaille

Abstract

Greater sage-grouse (*Centrocercus urophasianus*) are at the center of state and national land use policies largely because of their unique life-history traits as an ecological indicator for health of sagebrush ecosystems. This updated population trend analysis provides state and federal land and wildlife managers with best-available science to help guide current management and conservation plans aimed at benefitting sage-grouse populations. This analysis relied on previously published population trend modeling methodology from Coates and others (2021) and includes the addition of three analytical updates: (1) identification of population nadirs (lowest points within cycles) at the lek (breeding ground) and neighborhood cluster (group of leks) spatial scales, (2) truncation of prior distributions on rate of change in apparent abundance values to more realistic boundaries for leks with missing data, and (3) addition of 2 years of population lek count data (2020 and 2021) to the current dataset (1953–2021). Bayesian state-space models estimated 2.9 percent average annual decline in sage-grouse populations across their geographical range, which varied among subpopulations at the largest scale of analysis, termed climate clusters (2.2–4.6). Cumulative declines were 42.5, 65.6, and 80.1 percent range-wide across short (19 years), medium (35 years), and long (55 years) temporal periods, respectively. These results indicate that range-wide populations continued to decline during 2020 and 2021, although two climate clusters (eastern area and Bi-State area) have shown growth in population abundance in recent years, indicating they have surpassed a recent population abundance nadir.

Introduction

As of the turn of the twenty-first century, sage-grouse occupied roughly half of their former historical range (Schroeder and others, 2004; Miller and others, 2011) and populations have subsequently experienced marked declines in many parts of their current range (Garton and others, 2011; Western Association of Fish and Wildlife Agencies, 2015). In a recent study led by the U.S. Geological Survey (USGS), in collaboration with the Bureau of Land Management (BLM) and the Western Association of Fish and Wildlife Agencies (WAFWA), a Bayesian state-space modeling framework was used, which revealed an approximately 3.1-percent annual average decline range-wide that dates back to the 1960s (Coates and others, 2021). However, variation in trends was described across different spatial and temporal scales.

Decades of literature have attributed sage-grouse population declines to loss and fragmentation of sagebrush communities as well as to a suite of environmental stressors (Connelly and others, 2004; Schroeder and others, 2004; Doherty and others, 2016). Since 1999, sage-grouse have been petitioned for legal protection under the Endangered Species Act (ESA) on nine occasions, and actions to conserve and restore sage-grouse habitats are now central to guiding land-management actions and policies across most of the western United States. Specifically, in recent years, the resource needs of sage-grouse have been used to help guide management actions aimed at improving conditions in sagebrush ecosystems, with resultant practices thought to benefit other sagebrush-dependent species (Rowland and others, 2006; Hanser and Knick, 2011; Dinkins and others, 2021). Sage-grouse are considered an indicator for the function of sagebrush ecosystems and an umbrella for the protection of other sagebrush-obligate or semi-obligate species because of their near complete dependence on sagebrush ecosystems (Rich and Altman, 2001; Rich and others, 2005; Rowland and others, 2006; Hanser and Knick, 2011). However, some recent literature indicates that some less associated species might not be well covered by the sage-grouse umbrella (Carlisle and others, 2018). Importantly, several federal resource management plan amendments accompanying the U.S. Fish and Wildlife Service (USFWS) "not warranted" 2015 ESA listing determination called for greater integration of sage-grouse management into their land-use planning and specifically, for identifying how to implement adaptive management. An unprecedented level of conservation effort and planning among federal (Bureau of Land Management, 2015), state, and private stakeholders was identified as the primary driver for the USFWS decision in their most recent status assessment (U.S. Fish and Wildlife Service, 2015).

The purpose of this report is to provide updated results on sage-grouse population trends across their geographical range of western United States. This report reflects previous modeling efforts (1960–2019; Coates and others, 2021) and includes an additional 2 years of data (2020–21) to reflect the most current population trends. A detailed description of data collection and compilation, population clustering methods to identify spatial extents, and trend modeling methodologies were provided in the first three objectives described in Coates and others (2021). The USGS, in cooperation with the Western Association of Fish and Wildlife Agencies and Bureau of Land Management, are providing this scientific information to fulfill a prominent information gap that will help inform status assessments of sage-grouse population trends and conservation management strategies.

Study Area

Our study extent consisted of the geographic range of sage-grouse in the United States and was described previously in Coates and others (2021). Briefly, this area represents the sagebrush biome occurring across western North America and extending east from the Sierra Nevada/Cascade Mountain ranges to the western regions of the Great Plains of the United States. The vegetation communities vary with precipitation, temperature, soils, topographic position, and elevation (Miller and others, 2011). The most abundant shrub species include sagebrush (*Artemisia* spp.), with less abundant non-sagebrush species such as rabbitbrush (*Chrysothamnus* spp.), horsebrush (*Tetradymia* spp.), greasewood (*Sarcobatus* spp.), common snowberry (*Symphoricarpos* spp.), serviceberry (*Amelanchier* spp.), fourwing saltbush (*Atriplex* spp.), and bitterbrush (*Purshia* spp.). The primary herbaceous species include wheatgrass (*Agropyron* spp.), fescue (*Festuca* spp.), bluegrass (*Poa* spp.), needlegrass (*Stipa* spp.), bromegrass (*Bromus* spp.), and squirreltail (*Sitanion* spp.), whereas less abundant forb species include phlox (*Phlox* spp.), milk-vetch (*Astragalus* spp.), and fleabane (*Erigeron* spp.).

Data Compilation and Inputs

All digitized field observations of sage-grouse lek counts since 1953 were compiled from all state wildlife agencies that monitored sage-grouse populations and entered into a single unified database. We worked with each agency to ensure the fullest understanding of the data to maximize the number of appropriate records kept in the database, we addressed spatial errors, and we reviewed all data products with state wildlife staff members of the WAFWA Sage and Columbian Sharp-tailed Grouse Technical Committee. Data compilation rules and detailed methodology used in this analysis was published in Coates and others (2021) and O'Donnell and others (2021). The additional 2 years of data (2020 and 2021) used to update this trend analysis followed the exact quality assessment and quality control (QA/QC) measures described in the previous publications. Furthermore, state-specific summaries of number and percentage (relative to maximum value in any given year) of leks and observations retained followed the sequential application of Rules 1–6 described in appendix 2 of Coates and others (2021). Using all the rules for selecting data appropriate to population modeling, we retained 103,480 observations across 5,349 leks. The sage-grouse lek data used in this update either are not available or have limited availability owing to unique restrictions held by each state (data are managed by 11 western states and are not public due to the sensitivity of the species). Contact the Greater Sage-Grouse Technical Team of the Western Association of Fish and Wildlife Agencies or individual state wildlife agencies (see the "Acknowledgments" section) for more information.

Changes in population abundance are affected by environmental factors that operate on multiple spatial and temporal scales, which follow ecological, rather than geopolitical, boundaries. Hence, we examined population trends across biologically relevant and hierarchically nested units to improve the detection of factors driving change across various spatial scales. We grouped sage-grouse lek sites into hierarchical nested clusters or populations using least-cost minimum spanning trees, a clustering algorithm, and a suite of relevant biotic and abiotic spatial products described in Coates and others (2021). Briefly, we selected two cluster levels to represent a fine (neighborhood cluster, NC) and broad spatial scale (climate cluster, CC) in trend analyses. Model output included estimated abundance ($\widehat{N}$) and intrinsic rates of population change ($\hat{r}$) at the lek level.

Range-wide Sage-Grouse Population Model

Detailed formulation of the sage-grouse population model was described in Coates and others (2021). Briefly, we used a Bayesian state-space model (SSM) that relied on Markov chain Monte Carlo (MCMC) sampling to derive posterior probability distributions (PD) of $\widehat{N}$ and $\hat{r}$ using lek count data across the sage-grouse geographical range. This approach allowed inferences for each lek, as well as higher-order, and nested spatial extents such as NC and CC, during each year of the time series. Advantages and assumptions inherent to the SSM approach were described in Coates and others (2021). In the following paragraphs, we describe two analytical modifications to Coates and others (2021), representing an improvement from the original model and inferences. A third modification from the original analysis was the addition of 2 years of data (2020–21).

Modification 1—Priors on Missing Values

We modified our analysis to reflect more realistic sequences of $\hat{r}$ at lek locations where sampling was missed and data were unavailable; for example, not all leks were sampled every year of the time series, creating consecutive NAs in the encounter histories. Missing data were not an issue for modeling estimation when less than three consecutive NAs occurred. However, when a time series contained three or more consecutive NAs, inflated estimates of the upper credible interval (CRI) of $\widehat{N}$ could arise given the nature of the MCMC iterative process. Therefore, we improved the estimation of that lek-scale, derived parameter by truncating the prior distribution of $\hat{r}$ to fall within the range of −0.693–0.693 ($\hat{\lambda}$ = 0.5–2.0) when three or more consecutive NAs were observed. As such, $\widehat{N}$ was restricted to not decline by more than half or increase by more than double during the second of three consecutive years in which NA values existed. These values were established from realistic boundaries informed by data where leks were counted in subsequent years.

Modification 2—Identification of Population Nadirs

Accurate identification of population nadirs (lowest points within cycles) is fundamental to establishing temporal scales of inference across each of the spatial extents. We fully describe the purpose of making trend inferences across a series of years that align with population nadirs. Population trends at the lek and NC spatial scales were estimated using population nadirs at the climate cluster level in Coates and others (2021). Although we recognize advantages to this previous approach, it can lead to over- and under-estimation of $\hat{r}$ at the lek and NC level when nadirs are imperfectly aligned with their parent CC. During the initial analysis, visual identification of nadirs was not possible given the large amount of data (for example, greater than 30,000 nadir points across scales). Thus, we improved on the modeling inference by developing an algorithm (see description later in the text) that identified population nadirs from time series estimates of abundance on a population-by-population basis (in other words, for each lek or NC). Although nadirs at leks and NCs are closely aligned with those of CCs in many instances, slight shifts in years can improve accuracy in trends at the smaller spatial scales. This modification to the post-processing of PDs allowed for better accuracy in estimating these trends.

The steps of the algorithm were automated and reported in this section. The algorithm carried out a 5-year moving window during the time series of median abundance estimates. The initial placement of the window covered years 1960–64. Within the moving window, the year with the lowest abundance value was retained. The same process was repeated with a shift of 1 year for the initial start year. This process was carried out until all years had occupied the moving window at least one time, and the final location of the window covered years 2017–21. The subset of years that were identified as the low point within the moving window on greater than or equal to two occasions were isolated. That vector was referred to as intermediate nadirs #1 (*Inad*[1]). First and last years were automatically removed from consideration because these years could only be selected once within the moving window (in other words, first and last move of the sweep).

Working with $Inad^1$, all years that were within 3 years of a neighbor were identified; for example, if 1971 and 1973 were within $Inad^1$, both years would be identified as occurring within 3 years of a neighbor. Groups of neighbors were constructed using the same 3-year rule; for example, if in addition to 1971 and 1973, years 1975, 1979, and 1982 were within $Inad^1$; years 1971, 1973, and 1975 would belong to a group, and 1979 and 1982 would belong to a separate group. From those groups, only the year within each group that corresponded to the lowest abundance value for that group was retained. Thus, those years and all other years from $Inad^1$ that were greater than 3 years from a neighbor were retained. That vector was referred to as $Inad^2$.

$Inad^2$ was compared to the vector of CC nadirs that were visually identified during a preceding step and forced a one-to-one match based on the nearest years within each vector. If fewer years existed within $Inad^2$ compared to the vector of CC nadirs, all years within $Inad^2$ were retained. This vector was referred to as $Inad^3$.

Finally, median abundance estimates from 1960 and 2021 were compared to median abundance estimates corresponding to the first and last years from $Inad^3$, respectively. If the abundance value from 1960 or 2021 was lower than the abundance values associated with the first and last years from $Inad^3$, those years within the vector were replaced. That vector represented the final set of nadirs for the time series.

Modification 3—Two Additional Years of Data

The original version of this analysis included data from 1960 to 2019 (Coates and others, 2021). We have included two more years of data in the analysis for all 11 western states across sage-grouse geographic range. Because of the MCMC iterative processing, trend estimates before 2019 may experience slight shifts with the inclusion of the new data. This version of the analysis supersedes trends reported in Coates and others (2021) and represents current trends across different spatial extents (for instance, leks, NCs, and CCs) and temporal periods (for instance, 2021 back-in-time to each population nadir) across the geographic range of sage-grouse.

Range-wide Population Trends

Our model fit the observed data well (Bayesian p-value=0.51). Median $\widehat{N}$ from the SSM revealed six distinct range-wide population nadirs across the 62 years of data, which were 1966, 1975, 1986, 1996, 2002, and 2013. The range-wide, across-years, mean male count was 17.7 per lek (SD=23.5) based on data restricted to trend analyses. The number of years for complete oscillation periods (nadir-to-nadir) was relatively consistent across periods (average=9.4; 95-percent CRI=6.3–11.0; table 1). Model estimates revealed evidence of range-wide decline, on average, from every historic abundance nadir to 2021 (fig. 1; table 2); for example, the average annual $\hat{\lambda}$ for short (19 years, two oscillations), medium (35 years, four oscillations), and long (55 years, six oscillations) temporal scales was 0.971 (median; 95-percent CRI=0.969–0.973), 0.970 (median; 95-percent CRI=0.968–0.972), and 0.971 (median; 95-percent CRI=0.969–0.973), respectively. These trends imply declines of 42.5, 65.6, and 80.1 percent, relative to population sizes observed 19, 35, and 55 years earlier, respectively. In an earlier version of the model (Coates and others, 2021), we specified the final nadir for all populations using the final year of the dataset (2019), which was the lowest point of $\widehat{N}$ for most populations at that time. With the addition of 2 years of count data (2020–21), we have confirmed that 2019 was not a nadir for all populations modeled. As such, the previous conclusion of a positive rate of change (median $\hat{\lambda}$ >1) for CC-F (western Wyoming area) during recent (6 years, one oscillation) and short/medium (23 years, three oscillations) temporal scales has been changed to a negative rate of change (fig. 2). The five other CCs continued to demonstrate negative rates of change across all periods of oscillation, although some did exit their nadirs (CC-A, CC-D), showing signs of population growth during 2020–21. We estimated median $\hat{\lambda}$ to be less than 1.0 for 82.7, 86.2, and 96.7 percent of NCs across short, medium, and long temporal scales, respectively (fig. 3), throughout the sage-grouse range.

Table 1. Identified years of population abundance nadirs (lowest points within cycles) used to define temporal scales (recent to long-term) of population trend estimates across different climate clusters (A–F) and range-wide for greater sage-grouse (*Centrocercus urophasianus*) in the western United States.

[Range-wide estimated abundance nadirs were 1966, 1975, 1986, 1996, 2002, and 2013 that reflect long, medium/long, medium, short/medium, short, and recent, respectively, temporal scales for inferencing trends. **Abbreviations**: CC, climate cluster; A, Bi-State area; B, Washington area; C, Jackson Hole, Wyoming area; D, eastern area; E, Great Basin area; F, western Wyoming area]

CC	Long	Medium/ long	Medium	Medium/ short	Short	Recent
A	1969	1977	1983	1995	2002	2008
B	1964	1976	1987	1995	2001	2008
C	1963	1969	1984	1999	2003	2011
D	1966	1981	1986	1997	2004	2014
E	1967	1975	1985	1996	2002	2013
F	1967	1975	1987	1996	2002	2013
Range	1966	1975	1986	1996	2002	2013

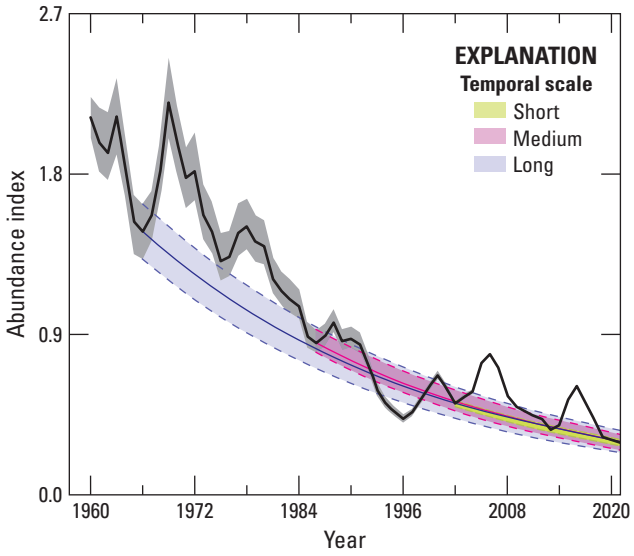

Figure 1. Abundance index (calculated as $\widehat{N}$ divided by 62-year mean of $\widehat{N}$) of greater sage-grouse (*Centrocercus urophasianus*) across their range from lek observations used to model population trends during 1960–2021. Median estimates (solid colored lines) and 95-percent credible limits (dashed colored lines) of abundance trend across temporal scales: Short (two periods), Medium (four periods), and Long (six periods), right to left. Black trend line represents median estimates. Colored areas represent 95-percent credible limits of trend estimates. Grey shaded areas represent 95-percent credible limits on abundance index.

Table 2. Greater sage-grouse (*Centrocercus urophasianus*) average annual rate of population change ($\hat{\lambda}$) across six different temporal scales that corresponded to differing periods of oscillation (recent [one period], short [two periods], short/medium [three periods], medium [four periods], medium/long [five periods], long [six periods]) for each climate cluster in western United States (see table 1).

[**Abbreviations**: CC, climate cluster; A, Bi-State area; B, Washington area; C, Jackson Hole, Wyoming area; D, eastern area; E, Great Basin area; F, western Wyoming area; $\hat{\lambda}$, estimated finite rate of population change]

CC	Temporal scales[1]						Number of leks[2]	Average count/lek[3]
	Long	Medium/long	Medium	Short/medium	Short	Recent		
A	0.978 (0.968–0.987)	0.980 (0.969–0.988)	0.989 (0.976–0.999)	0.992 (0.976–1.003)	0.976 (0.964–0.985)	0.988 (0.973–1.000)	90 (57)	20.5 (19.1–21.9)
B	0.954 (0.945–0.963)	0.949 (0.937–0.960)	0.948 (0.935–0.958)	0.957 (0.945–0.969)	0.963 (0.950–0.976)	0.955 (0.938–0.973)	111 (69)	13.9 (13.1–14.8)
C	0.966 (0.950–0.986)	0.967 (0.949–0.988)	0.969 (0.944–0.993)	0.971 (0.952–0.988)	0.965 (0.946–0.981)	0.945 (0.920–0.970)	17 (14)	13.6 (11.9–15.3)
D	0.967 (0.963–0.970)	0.960 (0.957–0.964)	0.968 (0.964–0.972)	0.981 (0.977–0.986)	0.961 (0.957–0.964)	0.979 (0.973–0.986)	3,021 (1,924)	16.1 (15.9–16.3)
E	0.972 (0.970–0.974)	0.974 (0.971–0.976)	0.974 (0.971–0.977)	0.983 (0.980–0.986)	0.968 (0.965–0.970)	0.950 (0.947–0.955)	4,114 (2,284)	16.4 (16.2–16.6)
F	0.975 (0.971–0.980)	0.973 (0.967–0.979)	0.971 (0.967–0.976)	0.989 (0.985–0.994)	0.976 (0.973–0.981)	0.975 (0.971–0.983)	1,269 (1,001)	22.9 (22.5–23.3)
Range	0.971 (0.969–0.973)	0.968 (0.966–0.970)	0.970 (0.968–0.972)	0.985 (0.983–0.987)	0.971 (0.969–0.973)	0.972 (0.969–0.975)	8,622 (5,349)	17.7 (17.5–17.8)

[1]Lengths of temporal scales were defined by population abundance nadirs that varied for each climate cluster (see table 1). Estimates for each period represent median $\hat{\lambda}$ with 95-percent credible intervals in parentheses.

[2]Number of leks in database and number that were used in analysis in parentheses.

[3]Average number of males counted on leks used in analysis and 95-percent confidence intervals in parentheses.

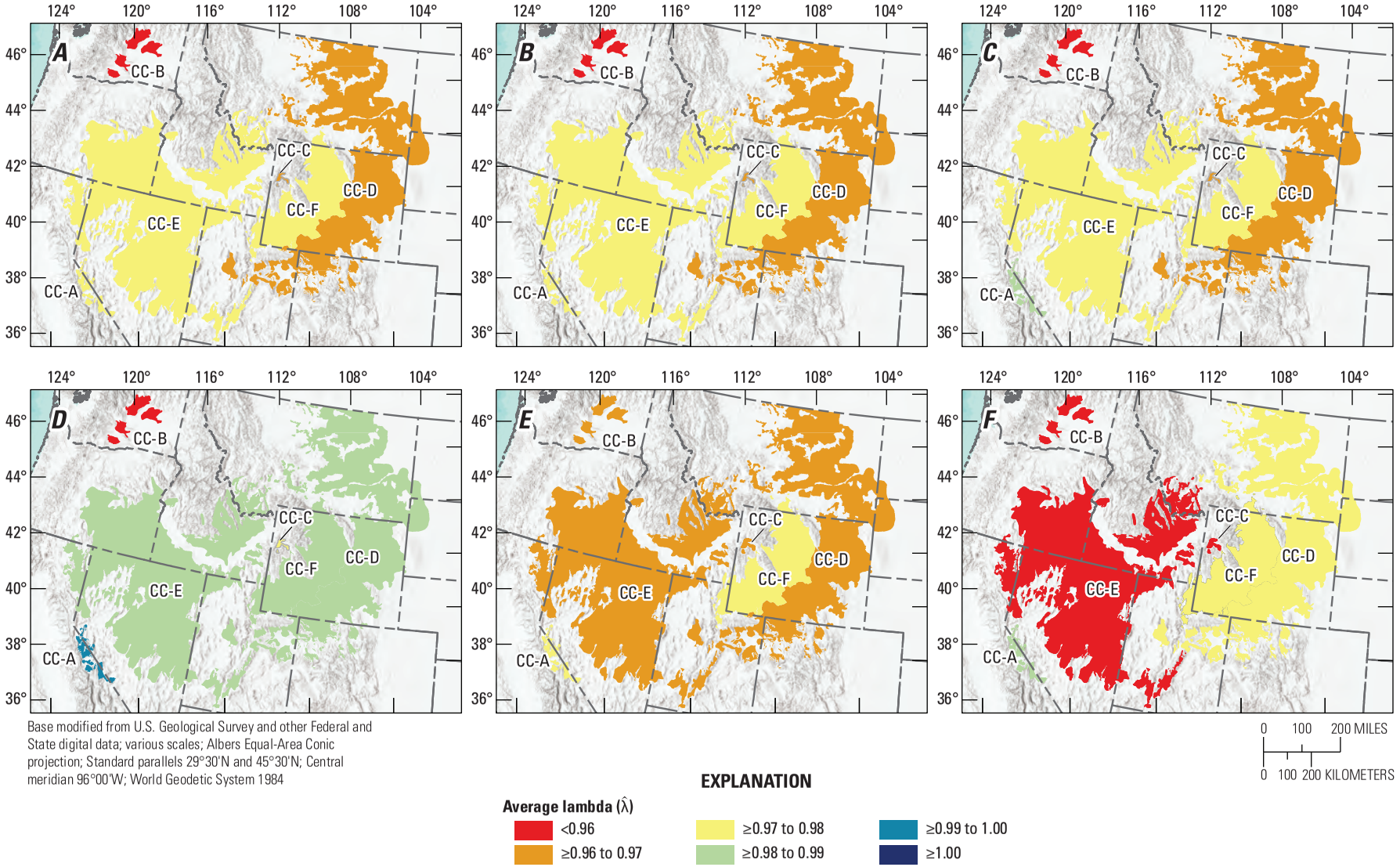

Climate clusters (Level 13): polygon colors represent average lambda ($\hat{\lambda}$) values of sage-grouse populations over six temporal scales. Approximately 30 percent of the distribution of average $\hat{\lambda}$ within the upper and lower color classes.

Figure 2. Range-wide spatial estimates of average annual rate of change ($\hat{\lambda}$) in abundance of greater sage-grouse (*Centrocercus urophasianus*) across six temporal scales based on periods of oscillation: *A*, Long (six periods); *B*, Medium/long (five periods); *C*, Medium (four periods); *D*, Short/medium (three periods); *E*, Short (two periods); and *F*, Recent (one period) for each climate cluster (CCs; A–F). Map image is the intellectual property of Esri and is used herein under license. Copyright © 2020 Esri and its licensors. All rights reserved. Abbreviations: <, less than; ≥, greater than or equal to.

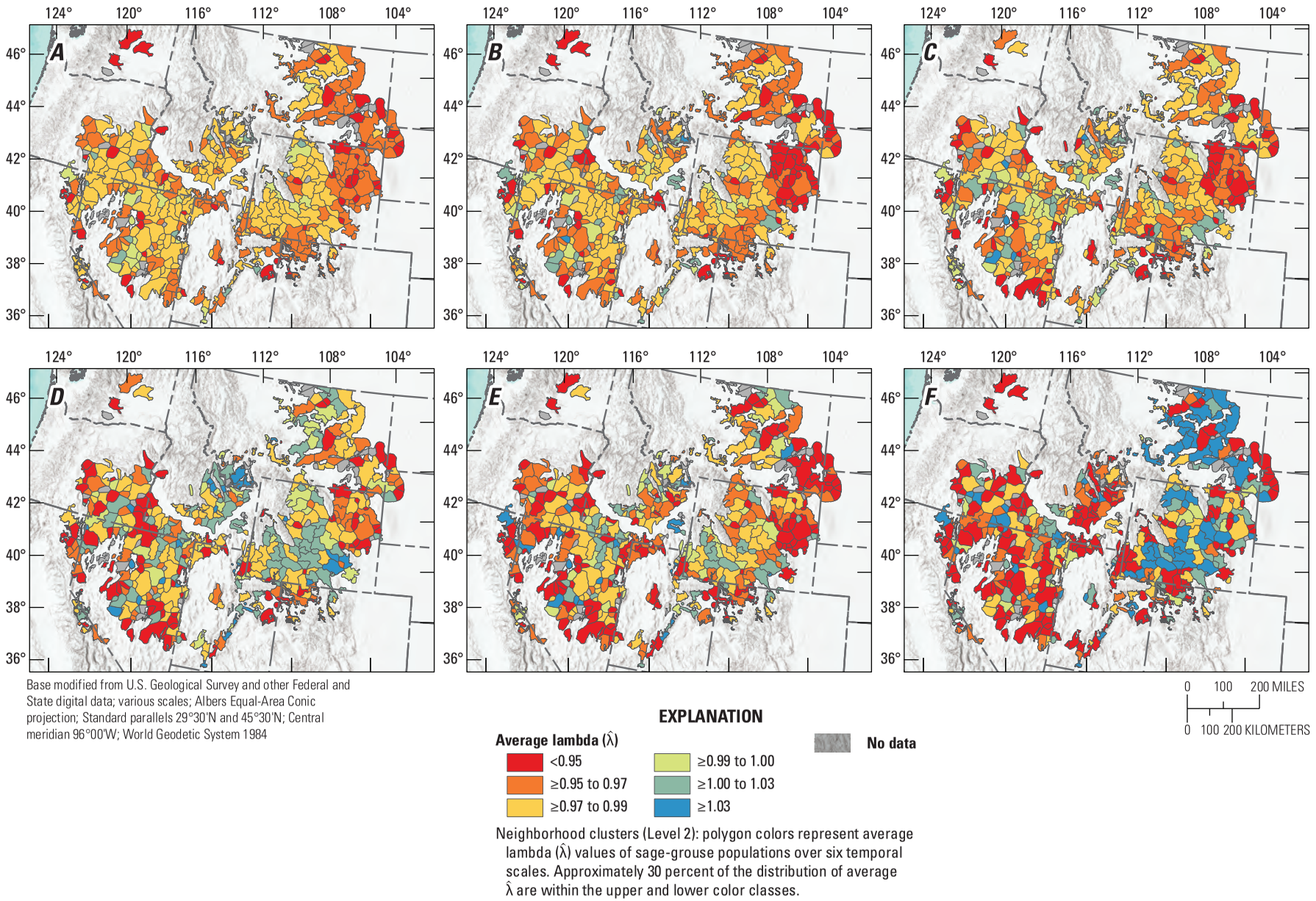

Figure 3. Range-wide spatial estimates of average annual rate of change ($\hat{\lambda}$) in abundance of greater sage-grouse (*Centrocercus urophasianus*) across six temporal scales based on periods of oscillation: *A*, Long (six periods); *B*, Medium/long (five periods); *C*, Medium (four periods); *D*, Short/medium (three periods); *E*, Short (two periods); and *F*, Recent (one period) for each neighborhood cluster. Map image is the intellectual property of Esri and is used herein under license. Copyright© 2020 Esri and its licensors. All rights reserved. Abbreviations: <, less than; ≥, greater than or equal to.

Climate Cluster Population Trends

Climate cluster A (CC-A; Bi-State area) consisted of 11 NCs that encompassed 726,907 hectares (ha). Two NCs did not have sufficient lek data to estimate trends. Climate cluster A consisted of 90 leks, representing approximately 1 percent of the range-wide database. After QA/QC, 57 leks met criteria for use in the SSM (table 2), totaling 1,630 field observations. Mean male count was 20.5 (95-percent confidence interval=19.1–21.9). For CC-A, we estimated six population abundance nadirs that dated back to 1960 and included nadirs of 1969, 1977, 1983, 1995, 2002, and 2008 (table 1). We estimated $\hat{\lambda}$ at the short (2002–21, two periods of oscillation over 17 years), medium (1983–2021, four periods over 36 years), and long temporal scales (1969–2021, six periods over 50 years) as 0.976 (95-percent CRI=0.964–0.985), 0.989 (95-percent CRI=0.976–0.999), and 0.978 (95-percent CRI=0.968–0.987), respectively (fig. 4*A*; table 2). Over the past 17, 36, and 50 years, sage-grouse populations have experienced declines in abundance equal to 34.0, 32.9, and 67.5 percent, respectively. We estimated median $\hat{\lambda}$ to be less than 1.0 for all NCs across short, medium, and long temporal scales, respectively.

Climate cluster B (CC-B; Washington area) consisted of four NCs that encompassed 726,907 ha. One NC did not have sufficient lek data to estimate trends. Climate cluster B consisted of 111 leks, representing approximately 1.3 percent of the lek database. After QA/QC, 69 leks met criteria for use in the state-space trend model (table 2), totaling 1,144 field observations. Mean male count was 13.9 (95-percent confidence interval=13.1–14.8). We estimated six population abundance nadirs that dated back to 1960 and included 1964, 1976, 1987, 1995, 2001, and 2008 (table 1). We estimated $\hat{\lambda}$ at the short (2001–21, two periods of oscillation over 20 years), medium (1987–2021, four periods over 34 years), and long-temporal scales (1964–2021, six periods over 57 years) as 0.963 (95-percent CRI=0.950–0.976), 0.948 (95-percent CRI=0.935–0.958), and 0.954 (95-percent CRI=0.945–0.963), respectively (fig. 4*B*; table 2). Over the past 20, 34, and 57 years, sage-grouse populations have experienced declines in abundance equal to 53.0, 84.0, and 93.2 percent, respectively. We estimated median $\hat{\lambda}$ to be less than 1.0 for all NCs across short, medium, and long temporal scales, respectively.

Climate cluster C (CC-C; Jackson Hole, Wyoming area) consisted of two NCs that encompassed 66,733 ha. Climate cluster C consisted of 17 leks, representing approximately 0.2 percent of the lek database. After QA/QC, 14 leks met criteria for use in the SSM (table 2), totaling 332 field observations. Mean male count was 13.6 (95-percent confidence interval=11.9–15.3). For CC-C, we estimated population abundance nadirs during 1963, 1969, 1984, 1999, 2003, and 2011 (table 1). We estimated $\hat{\lambda}$ at the short (2003–21, two periods of oscillation over 18 years), medium (1984–2021, four periods over 37 years), and long-temporal scales (1963–2021, six periods over 58 years) as 0.965 (95-percent CRI=0.946–0.981), 0.969 (95-percent CRI=0.944–0.993), and 0.966 (95-percent CRI=0.950–0.986), respectively. Over the past 18, 37, and 58 years, sage-grouse populations have experienced declines in abundance equal to 47.7, 68.5, and 86.4 percent, respectively (fig. 4*C*; table 2). We estimated median $\hat{\lambda}$ to be less than 1.0 for all NCs across this temporal scale.

Climate cluster D (CC-D; eastern area) consisted of 169 NCs that encompassed 25,920,530 ha. There were 24 NCs that did not have sufficient lek data for trend estimates. Climate cluster D consisted of 3,021 leks, representing approximately 35.0 percent of the lek database. After QA/QC, 1,924 leks met criteria for use in the SSM (table 2) and totaled 37,013 field observations. Mean male count was 16.1 (95-percent confidence interval=15.9–16.3). For CC-D, we estimated six population abundance nadirs that dated back to 1960 and included 1966, 1981, 1986, 1997, 2004, and 2014 (table 1). We estimated $\hat{\lambda}$ at the short (2004–21, two periods of oscillation over 15 years), medium (1986–2021, four periods over 33 years), and long temporal scales (1966–2021, six periods over 53 years) as 0.961 (95-percent CRI=0.957–0.964), 0.968 (95-percent CRI=0.964–0.972), and 0.967 (95-percent CRI=0.963–0.970), respectively (fig. 4*D*; table 2). Over the past 15, 33, and 53 years, sage-grouse populations have experienced declines in abundance equal to 45.0, 65.8, and 83.5 percent, respectively. We estimated median $\hat{\lambda}$ to be less than 1.0 for 86.9, 94.5, and 99.3 percent of NCs across short, medium, and long temporal scales, respectively.

Climate cluster E (CC-E; Great Basin area) consisted of 241 NCs that encompassed 34,627,182 ha. There were 25 NCs that lacked sufficient data to estimate trends. Climate cluster E consisted of 4,114 leks, representing approximately 47.7 percent of the lek database. After QA/QC, 2,284 leks met criteria for use in the SSM (table 2) and totaled 41,732 field observations. Mean male count was 16.4 (95-percent confidence interval=16.2–16.6). For CC-E, we estimated six population abundance nadirs that dated back to 1960 and included 1967, 1975, 1985, 1996, 2002, and 2013 (table 1). We estimated $\hat{\lambda}$ at the short (2002–21, two periods of oscillation over 19 years), medium (1985–2021, four periods over 36 years), and long temporal scales (1967–2021, six periods over 54 years) as 0.968 (95-percent CRI=0.965–0.970), 0.974 (95-percent CRI=0.971–0.977), and 0.972 (95-percent CRI=0.970–0.974), respectively (fig. 4*E*; table 2). Over the past 19, 36, and 54 years, sage-grouse populations have experienced declines in abundance equal to 46.4, 61.4, and 78.6 percent, respectively. We estimated median $\hat{\lambda}$ to be less than 1.0 for 80.1, 79.6, and 95.4 percent of NCs across short, medium, and long temporal scales, respectively.

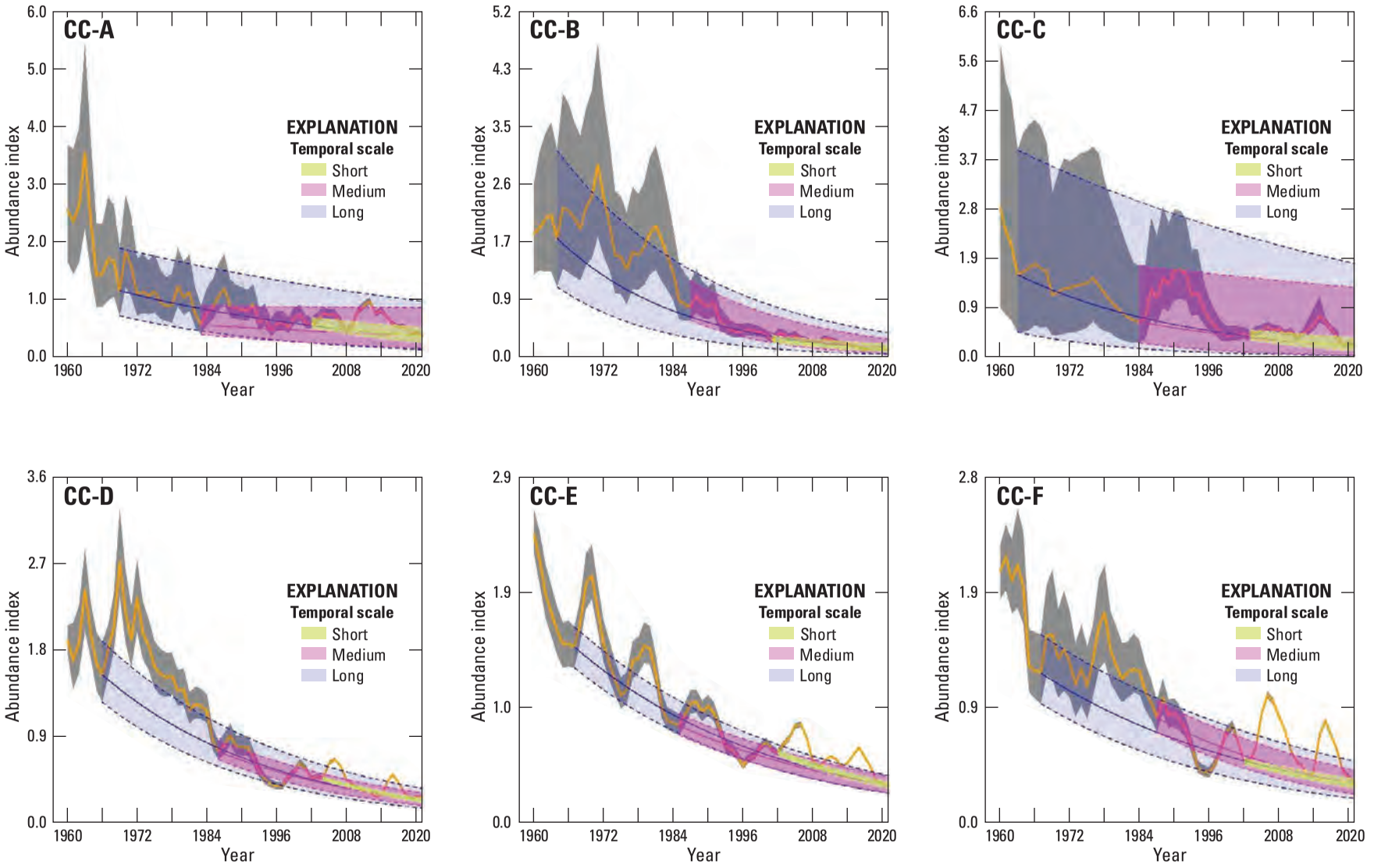

Figure 4. Abundance index (calculated as $\widehat{N}$ divided by 62-year mean of $\widehat{N}$) of greater sage-grouse (*Centrocercus urophasianus*) in climate clusters (CCs) *A* (CC-A; Bi-State area); *B* (CC-B; Washington area); *C* (CC-C; Jackson Hole, Wyoming area); *D* (CC-D; Eastern area); *E* (CC-E; Great Basin area); and *F* (CC-F; western Wyoming area). Lek observations were used to model population trends during 1960–2021. Median estimates (solid colored lines) and 95-percent credible limits (dashed colored lines) of abundance trends across temporal scales based on periods of oscillation: Short (two periods), Medium (four periods), and Long (six periods), right to left. Colored areas represent 95-percent credible limits of trend estimates. Black lines and grey shaded areas represent median and 95-percent credible limits on abundance index, respectively.

Climate cluster F (CC-F; western Wyoming area) consisted of 56 NCs that encompassed 8,899,755 ha. Three NCs lacked sufficient data to estimate trends. Climate cluster F consisted of 1,269 leks, representing approximately 14.7 percent of the lek database. After QA/QC, 1,001 leks met criteria for inclusion in the SSM (table 2) and totaled 21,629 field observations. Mean male count was 22.9 (95-percent confidence interval=22.5–23.3). For CC-F, we estimated six population abundance nadirs that dated back to 1960 and included 1967, 1975, 1987, 1996, 2002, and 2013 (table 1). We estimated $\hat{\lambda}$ at the short (2002–21, two periods of oscillation over 19 years), medium (1987–2021, four periods over 34 years), and long temporal scales (1967–2021, six periods over 54 years) as 0.976 (95-percent CRI=0.973–0.981), 0.971 (95-percent CRI=0.967–0.976), and 0.975 (95-percent CRI=0.971–0.980), respectively (fig. 4*F*; table 2). Over the past 19, 34, and 54 years, sage-grouse populations have experienced declines in abundance equal to 36.9, 63.2, and 74.2 percent, respectively. We estimated median $\hat{\lambda}$ to be less than 1.0 for 77.4, 86.8, and 94.3 percent of NCs across short, medium, and long temporal scales, respectively.

Neighborhood cluster trends for different temporal scales that are not listed in this report can be found in Coates and others (2022). Coates and others (2022) is the accompanying data release to this report.

Watches and Warnings from a Targeted Annual Warning System

The Targeted Annual Warning System (TAWS) is a hierarchical monitoring strategy that contrasts estimates of $\hat{r}$ across nested spatial scales on an annual basis. Comparisons can act as a powerful analytical tool to help target when and where to carry out management actions. Part of the system includes an annual report of signals referred to as watches and warnings, which signify progressively greater degrees of evidence for abnormal decline. Evidence of abnormal decline is assessed using independent sets of standardized thresholds that seek to stabilize the range-wide population (range-wide thresholds) versus individual climate clusters (climate cluster thresholds). The original report presented TAWS results from each set of thresholds to provide managers with multiple strategic options. Here, we chose to report TAWS results using CC thresholds based on feedback of implementation from state and federal agency personnel. The primary reason for preferential use of CC thresholds is the superior performance in targeting peripheral and sparsely distributed populations. Like the trend analysis, thousands of historic lek surveys underwent QA/QC, as described in the results of Objective 1 for the TAWS analysis (Coates and others, 2021). During 1990–2021, we estimated 0.651 and 0.494 proportion of sage-grouse leks experienced watches and warnings (table 3; fig. 5), respectively, across the range. We calculated a mean annual proportion of leks that underwent first watches and warnings to be 0.024 (repeat=0.060) and 0.018 (repeat=0.059), respectively, which is approximately 111 (repeat=278) and 84 (repeat=271) leks each year. The CC with greatest proportion of activated watches at leks across the 31 years was CC-A (Bi-State area), where 0.896 proportion of leks activated one or more times (table 3). Conversely, CC-E consisted of the greatest number of watches compared to other clusters (number of first watches=1,271, number of repeat watches=3,175; table 3). The CC with the least proportion of watches was CC-B (Washington area), at 0.435 (number of first and repeat watches=20 and 73, respectively; table 3). The CC with the greatest proportion (0.688) of warnings was CC-A, whereas CC-E had the greatest number (first=956 and repeat=3,153). The second highest proportion of watches (0.844) and warnings (0.619) was CC-F (western Wyoming area), where we estimated 771 (repeat=2,407) and 565 (repeat=2,042), respectively, during this timeframe.

We estimated 0.525 and 0.332 proportion of NCs were activated as first watches and warnings (table 3; fig. 6), respectively, at NCs range-wide during 1990–2021. An average of 0.019 (repeat=0.048) and 0.012 (repeat=0.034) proportion of clusters activated per year, which was approximately 8.1 (repeat=19.9) and 5.1 (repeat=14.0) clusters. We reported CC-A (Bi-State area) had the greatest proportion (1.000) of watches, whereas CC-E (Great Basin area) had the greatest number (first=158 and repeat=415) of watches across the 31-year timeframe. For warnings, CC-E had the greatest number (first=98 and repeat=287) and CC-A had the greatest proportion (0.556; table 3).

During 2021, we estimated 0.028 and 0.023 proportion of leks experienced first watches and warnings, respectively, range-wide (table 4), which resulted in 127 (repeat=420) and 104 (repeat=489) lek activations. During 2021, the greatest proportion of first watches (0.047) and warnings (0.031) were within CC-E, which were 91 (repeat=222) watches and 60 (repeat=216) warnings (table 4). Climate clusters A–C had no lek-level watches activated during 2021, but CC-A did experience one first warning (table 4). We estimated 0.048 and 0.036 proportion of neighborhoods experienced first watches and warnings, respectively, range-wide in 2021 (table 4). Climate cluster A had the highest proportion of first watches in 2021 (0.111), whereas CC-E experienced the greatest proportion of NC warnings (0.056). Warnings and watches for each neighborhood cluster are available in Coates and others (2022).

Table 3. Watches and warnings identified at greater sage-grouse (*Centrocercus urophasianus*) leks and neighborhood clusters (NC) across climate clusters (A–F) using state-space model estimates within a targeted annual warning system in the western United States during 1990–2021. Number of watches and warnings that include repeat (r), only first time (f), and proportion (p) of populations (lek or NC) are reported.

[Number of watches and warnings that include repeat (r), only first time (f), and proportion (p) of populations (lek or NC) are reported. **Abbreviations**: CC, climate cluster; A, Bi-State area; B, Washington area; C, Jackson Hole, Wyoming area; D, eastern area; E, Great Basin area; F, western Wyoming area]

CC	Level	r.watch	f.watch	p.watch	r.warning	f.warning	p.warning	Total
A	Lek	196	43	0.896	161	33	0.688	48
B	Lek	73	20	0.435	92	20	0.435	46
C	Lek	40	8	0.571	36	7	0.500	14
D	Lek	1,601	889	0.543	1,834	694	0.424	1,636
E	Lek	3,175	1,271	0.651	3,153	956	0.490	1,952
F	Lek	2,407	771	0.844	2,042	565	0.619	913
Total	Lek	7,492	3,002	0.651	7,318	2,275	0.494	4,609
A	NC	41	9	1.000	22	5	0.556	9
B	NC	5	1	0.500	2	1	0.500	2
C	NC	6	1	0.500	7	1	0.500	2
D	NC	29	21	0.150	45	23	0.164	140
E	NC	415	158	0.742	287	98	0.460	213
F	NC	43	30	0.566	16	11	0.208	53
Total	NC	539	220	0.525	379	139	0.332	419

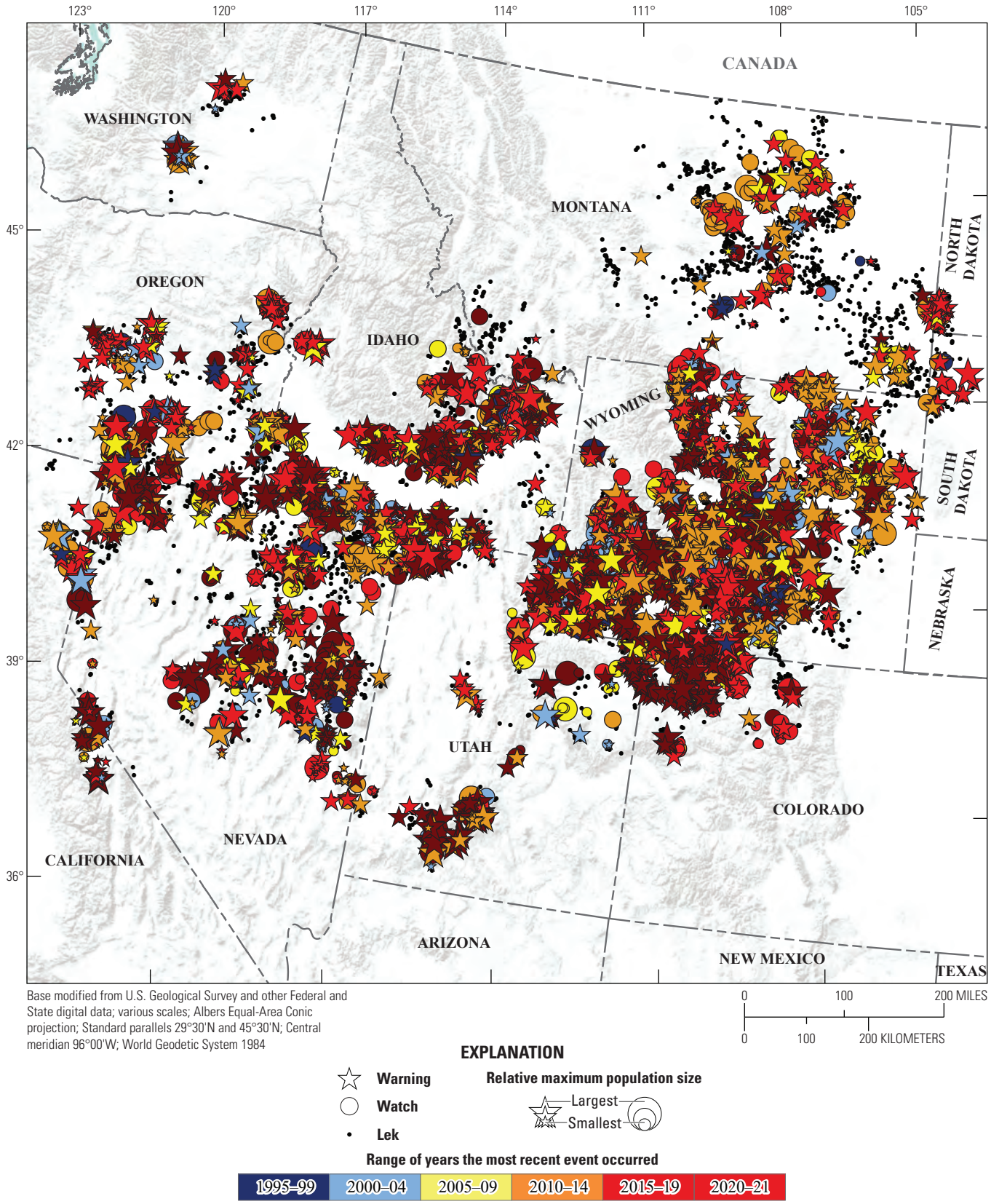

Figure 5. Spatial and temporal depiction of range-wide watches and warnings of greater sage-grouse (*Centrocercus urophasianus*) population declines at the lek scale in the western United States from 1990 to 2021. Map image is the intellectual property of Esri and is used herein under license. Copyright© 2020 Esri and its licensors. All rights reserved.

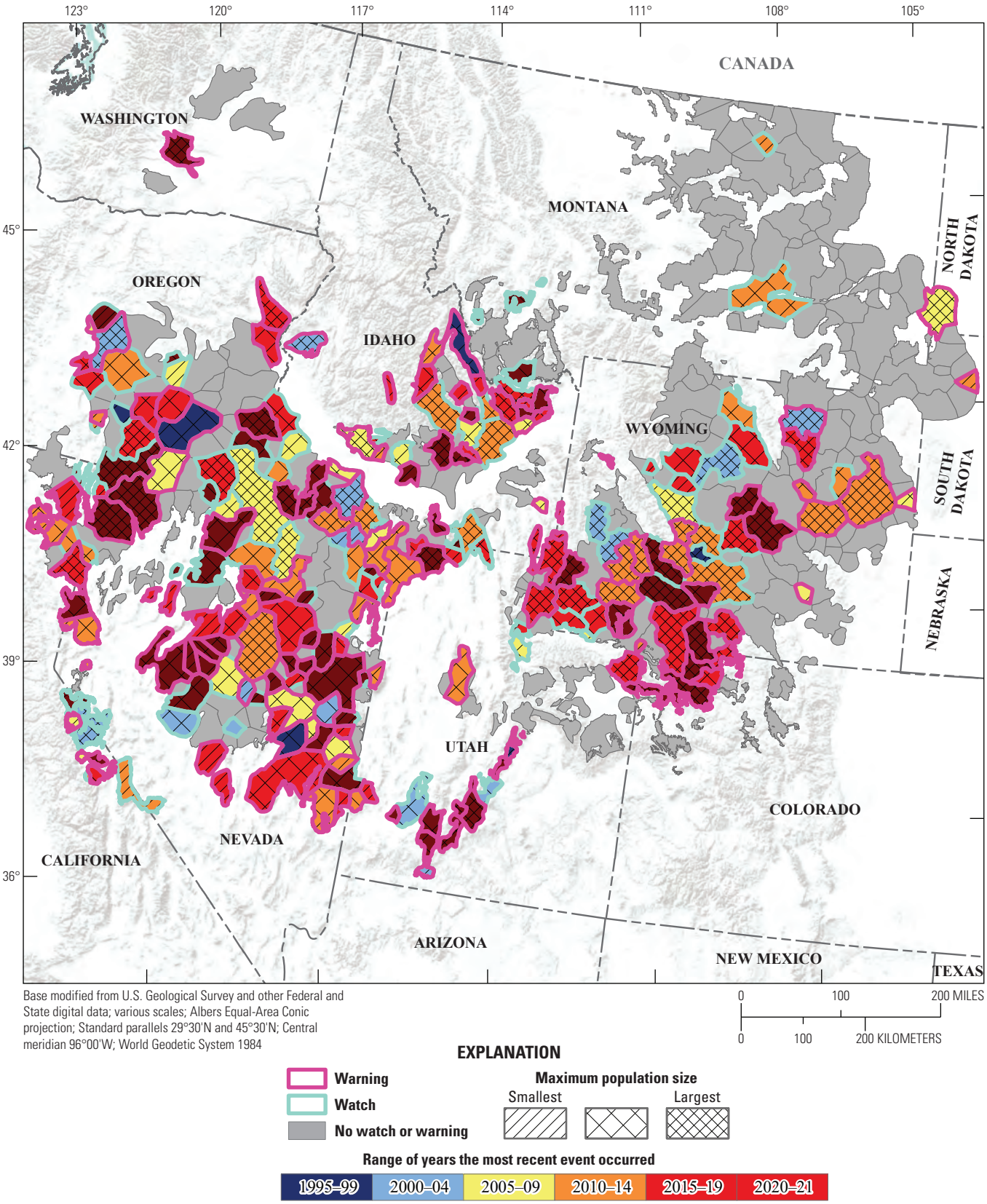

Figure 6. Spatial and temporal depiction of range-wide watches and warnings of greater sage-grouse (*Centrocercus urophasianus*) population declines at the neighborhood cluster scale in the western United States from 1990 to 2021. Map image is the intellectual property of Esri and is used herein under license. Copyright © 2020 Esri and its licensors. All rights reserved.

Table 4. Watches and warnings identified at the lek and neighborhood cluster (NC) scales across different climate clusters (A–F) by state-space model estimates using a targeted annual warning system framework for greater sage-grouse (*Centrocercus urophasianus*) across their range in the western United States during 2021. Number of watches and warnings that include repeat (r), only first time (f), and proportion (p) of populations (lek or NC) are reported.

[Number of watches and warnings that include repeat (r), only first time (f), and proportion (p) of populations (lek or NC) are reported. **Abbreviations**: CC, climate cluster; A, Bi-State area; B, Washington area; C, Jackson Hole, Wyoming area; D, eastern area; E, Great Basin area; F, western Wyoming area]

CC	Level	r.watch	f.watch	p.watch	r.warning	f.warning	p.warning	Total
A	Lek	8	0	0.000	13	1	0.021	48
B	Lek	0	0	0.000	2	0	0.000	46
C	Lek	1	0	0.000	1	0	0.000	14
D	Lek	67	22	0.013	113	18	0.011	1,636
E	Lek	222	91	0.047	216	60	0.031	1,952
F	Lek	122	14	0.015	144	25	0.027	913
Total	Lek	420	127	0.028	489	104	0.023	4,609
A	NC	1	1	0.111	1	0	0.000	9
B	NC	0	0	0.000	1	0	0.000	2
C	NC	0	0	0.000	0	0	0.000	2
D	NC	2	0	0.000	3	1	0.007	140
E	NC	43	18	0.085	27	12	0.056	213
F	NC	3	1	0.019	2	2	0.038	53
Total	NC	49	20	0.048	34	15	0.036	419

References Cited

Bureau of Land Management, 2015, Notice of availability of the record of decision and approved resource management plan amendments for the Great Basin Region greater sage-grouse sub-regions of Idaho and southwestern Montana; Nevada and northeastern California; Oregon; and Utah—Department of the Interior, Bureau of Land Management: Federal Register, v. 80, p. 57633–57635, accessed August 15, 2022, at https://www.federalregister.gov/documents/2015/09/24/2015-24213/notice-of-availability-of-the-record-of-decision-and-approved-resource-management-plan-amendm.

Carlisle, J.D., Keinath, D.A., Albeke, S.E., and Chalfoun, A.D., 2018, Identifying holes in the greater sage-grouse conservation umbrella: The Journal of Wildlife Management, v. 82, no. 5, p. 948–957. [Available at https://doi.org/10.1002/jwmg.21460].

Coates, P.S., Prochazka, B.G., O'Donnell, M.S., Aldridge, C.L., Edmunds, D.R., Monroe, A.P., Ricca, M.A., Wann, G.T., Hanser, S.E., Wiechman, L.A., and Chenaille, M.P., 2021, Range-wide greater sage-grouse hierarchical monitoring framework—Implications for defining population boundaries, trend estimation, and a targeted annual warning system: U.S. Geological Survey Open File Report 2020–1154, 243 p., accessed August 15, 2022, at https://doi.org/10.3133/ofr20201154.

Coates, P.S., Prochazka, B.G., Aldridge, C.L., O'Donnell, M.S., Edmunds, D.R., Monroe, A.P., Hanser, S.E., Wiechman, L.A., and Chenaille, M.P., 2022, Trends and a targeted annual warning system for greater sage-grouse in the western United States (1960–2021): U.S. Geological Survey data release, https://doi.org/10.5066/P9OQWGIV.

Connelly, J.W., Knick, S.T., Schroeder, M.A., and Stiver, S.J., 2004, Conservation assessment of greater sage-grouse and sagebrush habitats: Cheyenne, Wyo., Western Association of Fish and Wildlife Agencies, 611 p., accessed August 15, 2022, at https://wdfw.wa.gov/sites/default/files/publications/01118/wdfw01118.pdf.

Dinkins, J.B., Lawson, K.J., and Beck, J.L., 2021, Influence of environmental change, harvest exposure, and human disturbance on population trends of greater sage-grouse: PLoS One, v. 16, no. 9, p. e0257198. [Available at https://doi.org/10.1371/journal.pone.0257198].

Doherty, K.E., Evans, J.S., Coates, P.S., Juliusson, L.M., and Fedy, B.C., 2016, Importance of regional variation in conservation planning—A rangewide example of the greater sage-grouse: Ecosphere, v. 7, no. 10, p. 1–27, accessed August 15, 2022, at https://doi.org/10.1002/ecs2.1462.

Garton, E.O., Connelly, J.W., Horne, J.S., Hagen, C.A., Moser, A., and Schroeder, M., 2011, Greater sage-grouse population dynamics and probability of persistence, *in* Knick, S.T., and Connelly, J.W., eds., Greater sage-grouse—Ecology and conservation of a landscape species and its habitats: Berkeley, Calif., University of California Press, Studies in Avian Biology, v. 38, p. 292–381, accessed August 15, 2022, at https://doi.org/10.1525/california/9780520267114.003.0016.

Hanser, S.E., and Knick, S.T., 2011, Greater sage-grouse as an umbrella species for shrubland passerine birds—A multiscale assessment, *in* Knick, S.T., and Connelly, J.W., eds., Greater sage-grouse—Ecology and conservation of a landscape species and its habitats: Berkeley, Calif., University of California Press, Studies in Avian Biology, v. 38, p. 474–487, accessed August 15, 2022, at https://doi.org/10.1525/california/9780520267114.003.0020.

Miller, R.F., Knick, S.T., Pyke, D.A., Meinke, C.W., Hanser, S.E., Wisdom, M.J., and Hild, A.L., 2011, Characteristics of sagebrush habitats and limitations to long-term conservation, *in* Knick, S.T., and Connelly, J.W., eds., Greater sage-grouse—Ecology and conservation of a landscape species and its habitats: Berkeley, Calif., University of California Press, Studies in Avian Biology, v. 38, p. 144–184, accessed August 15, 2022, at https://doi.org/10.1525/california/9780520267114.003.0011.

O'Donnell, M.S., Edmunds, D.R., Aldridge, C.L., Heinrichs, J.A., Monroe, A.P., Coates, P.S., Prochazka, B.G., Hanser, S.E., Wiechman, L.A., Christiansen, T.J., Cook, A.A., Espinosa, S.P., Foster, L.J., Griffin, K.A., Kolar, J.L., Miller, K.S., Moser, A.M., Remington, T.E., Runia, T.J., Schreiber, L.A., Schroeder, M.A., Stiver, S.J., Whitford, N.I., and Wightman, C.S., 2021, Synthesizing and analyzing long-term monitoring data—A greater sage-grouse case study: Ecological Informatics, v. 63, p. 101327. [Available at https://doi.org/10.1016/j.ecoinf.2021.101327].

Rich, T., and Altman, B., 2001, Under the sage-grouse umbrella: Bird Conservation, v. 14, 10 p.

Rich, T.D., Wisdom, M.J., and Saab, V.A., 2005, Conservation of sagebrush steppe birds in the interior Columbia Basin, General Technical Report PSW-GTR-191, *in* Ralph, C.J., Rich, T., and Long, L., eds., Proceedings of the third international partners in flight conference: Albany, Calif., U.S. Department of Agriculture, Forest Service, Pacific Southwest Research Station, p. 589–606.

Rowland, M.M., Wisdom, M.J., Suring, L.H., and Meinke, C.W., 2006, Greater sage-grouse as an umbrella species for sagebrush-associated vertebrates: Biological Conservation, v. 129, no. 3, p. 323–335, accessed August 15, 2022, at https://doi.org/10.1016/j.biocon.2005.10.048.

Schroeder, M.A., Aldridge, C.L., Apa, A.D., Bohne, J.R., Braun, C.E., Bunnell, S.D., Connelly, J.W., Deibert, P.A., Gardner, S.C., Hilliard, M.A., Kobriger, G.D., McAdam, S.M., McCarthy, C.W., McCarthy, J.J., Mitchell, D.L., Rickerson, E.V., and Stiver, S.J., 2004, Distribution of sage-grouse in North America: The Condor, v. 106, no. 2, p. 363–376, accessed August 15, 2022, at https://doi.org/10.1093/condor/106.2.363.

U.S. Fish and Wildlife Service, 2015, Endangered and threatened wildlife and plants; 12-month finding on a petition to list greater sage-grouse (*Centrocercus urophasianus*) as an endangered or threatened species: Federal Register, v. 80, no. 191, p. 59857–59942, accessed August 15, 2022, at https://www.govinfo.gov/content/pkg/FR-2015-10-02/pdf/2015-24292.pdf.

Western Association of Fish and Wildlife Agencies, 2015, Greater sage-grouse population trends: An analysis of lek count databases 1965–2015: Cheyenne, Wyo., Western Association of Fish and Wildlife Agencies, 55 p., accessed August 15, 2022, at https://ir.library.oregonstate.edu/concern/technical_reports/ng451p621.

For more information concerning the research in this report, contact the Director, Western Ecological Research Center

U.S. Geological Survey
3020 State University Drive East
Sacramento, California 95819
https://www.usgs.gov/centers/werc

Publishing support provided by the U.S. Geological Survey
Science Publishing Network, Sacramento Publishing Service Center

ISSN 2771-9448 (online)
https://doi.org/10.3133/dr1165